Large nonvolatile multiple-state resistive switching in $TiO_{2-\delta}$/PMN-PT field-effect device

Hao Ni,[1,2,a)] Ming Zheng,[2,a)] Liping Chen,[3] Weiyi Huang,[2] Yaping Qi,[2] Jiali Zeng,[2] Zhenhua Tang,[2] Huibin Lu,[4] and Ju Gao[2,a)]
[1]*College of Science, China University of Petroleum, Qingdao 266580, China*
[2]*Department of Physics, The University of Hong Kong, Pokfulam Road, Hong Kong, China*
[3]*Department of Physics, Zhejiang Normal University, Jinhua 321004, China*
[4]*Institute of Physics, Chinese Academy of Sciences, Beijing 100190, China*

(Received 2 March 2017; accepted 14 May 2017; published online 25 May 2017)

$TiO_{2-\delta}$ thin films were epitaxially grown on (001)-oriented 0.7Pb($Mg_{1/3}Nb_{2/3}$)O_3-0.3$PbTiO_3$ (PMN-PT) ferroelectric single-crystal substrates. By applying electric fields E across the PMN-PT, the $TiO_{2-\delta}$ film resistance could be reversibly switched into different stable states at room temperature. The on-off ratio, tuned by the strength of the electric field E, remained at ∼1 under the $E \leq 0.6$ kV/cm and reached ∼3413 with the E increasing to 6 kV/cm, leading to a promising approach for designing nonvolatile multiple-state memory devices. By taking into account the migration of the oxygen vacancies and the ferroelectric field effect induced charge manipulations, the mechanism of the multiple-state resistive switching behaviors was discussed. *Published by AIP Publishing.*
[http://dx.doi.org/10.1063/1.4984218]

Over the past few years, nonvolatile, fast, and low power-consumed random access memory (RAM) has attracted considerable interest for its tremendous application in the electronic industry. Ferroelectric-based heterostructures, where nonvolatile ferroelectric (FE) polarization states −P and +P can be switched by electric fields directly, are one promising candidate.[1–7] One approach is the ferromagnetic/ferroelectric (FM/FE) multiferroic heterostructures which can realize electric field controlling of magnetism using the magnetoelectric coupling effect.[8] Furthermore, the corresponding multiferroic tunnel junctions (FM/thin-FE/FM) have been proposed to be for four-state devices as the result of the coexistence of tunneling magnetoresistance and tunneling electroresistance.[9,10] However, the sophisticated microstructure and the good performances limited by low temperature are technological challenges for device applications. Recently, the strain effect on the ferroelectric 0.7Pb($Mg_{1/3}Nb_{2/3}$)O_3–0.3$PbTiO_3$ (PMN-PT) has been utilized independently for nonvolatile storage.[11–18] The electric field induced strain in the ferroelectric layer was *in-situ* transferred to its epitaxial film, thus switching magnetization and resistance of the films. By applying electric fields on the PMN-PT, metastable ferroelastic strains have been achieved, leading to the nonvolatile and reversible resistive switching.[16–18] Nonetheless, the strain-induced resistance modulations [Fe_3O_4/PMN-PT ($\Delta\rho/\rho \sim 2.3\%$)[16] and VO_2/PMN-PT ($\Delta\rho/\rho \sim 10.7\%$)[18]] at room temperature are quite small and unsuited to practical application. On the other hand, the ferroelectric-based field effect transistor (FeFET), offering the reversible and nonvolatile resistive switching due to dual remnant polarization in the absence of an externally applied electric field, is also an effective way to fabricate ferroelectric storage devices.[19,20] The reversible ferroelectric polarization attracts or repels charge carriers, creating a thin charge accumulation or depletion channel at the interface and therefore modifies the charge-related electronic transport properties. In the oxide/FE FeFET structure, as a channel material a correlated oxide shows high resistance modulations ($La_{1-x}Ca_xMnO_3$/$PbZr_{0.2}Ti_{0.8}O_3$ [$\Delta\rho/\rho \sim 300\%$)[21] and ZnO:Mn/PMN-PT ($\Delta\rho/\rho \sim 53\%$)[22]] because electronic transport properties are sensitive to the charge carrier concentration. An additional advantage for the oxide/FE FeFET structure is that the high carrier concentration of the oxide channel (∼10^{21} cm^{-3}) reduces the depolarization field and thus improves the retention time.[2]

$TiO_{2-\delta}$, whose electronic transport properties are sensitive to the charge carrier concentration, is a promising channel material for the oxide/FE FeFET. Moreover, the migration of oxygen vacancies can significantly change resistance of the $TiO_{2-\delta}$ film which makes the $TiO_{2-\delta}$ film one of the important materials for nonvolatile resistive switching memory devices. By combining the resistive switching properties of the $TiO_{2-\delta}$ film and the ferroelectric field effect from the ferroelectric substrate, we fabricate a FeFET structure composed of a ferroelectric single crystal (001)-0.7Pb($Mg_{1/3}Nb_{2/3}$)O_3-0.3$PbTiO_3$ (PMN-PT) substrate and an epitaxial 40 nm-thick oxygen deficient $TiO_{2-\delta}$ film. In such a FeFET structure, the gate voltage tunable effect on resistance of the $TiO_{2-\delta}$ film has been studied at room temperature. By applying sweeping electric fields across the PMN-PT, the film resistance could be reversibly modulated into different stable states and the modulations (R_{OFF}/R_{ON} ∼3413 at 6 kV/cm) are much larger than those of other reported transition-metal oxide film/PMN-PT heterostructures.[16,18,22] The mechanism is discussed due to the migration of the oxygen vacancies and charge manipulation by the ferroelectric polarization switching. The nonvolatile, multiple-state and reproducible resistive switching behavior in $TiO_{2-\delta}$/PMN-PT at room temperature presents a potential strategy for designing nonvolatile memory devices.

The $TiO_{2-\delta}$ thin film was grown on the (001)-oriented PMN-PT single crystal substrate with 3×5 mm^2 size and 0.5 mm thickness by a pulsed laser deposition technique. A

a)nihao@upc.edu.cn; zhengm@mail.ustc.edu.cn; and jugao@hku.hk

0003-6951/2017/110(21)/213503/5/$30.00 Published by AIP Publishing.

high purity TiO_2 (99.99%) ceramic disk was used as the target and ablated by a KrF excimer laser (248 nm) with a laser energy density of 1.5 J/cm^2 and a repetition rate of 2 Hz. Film deposition was carried out at 700 °C under the oxygen pressure of 0.5 Pa. The thickness of the $TiO_{2-\delta}$ film was ~40 nm controlled via the deposition time. After deposition, the sample was annealed *in-situ* at 700 °C under 0.5 Pa oxygen pressure for ~10 min and 1000 Pa oxygen pressure for ~10 min, sequentially. After that, the sample was cooled to room temperature in an oxygen atmosphere naturally.

X-ray diffraction (XRD) was adopted to measure the crystallographic properties of the $TiO_{2-\delta}$ film. Figure 1 shows the typical θ-2θ XRD pattern of the $TiO_{2-\delta}$/PMN-PT structure. Except for the (00*l*) diffraction peaks from the pseudo-cubic PMN-PT substrate ($a \sim b \sim c = 4.02$ Å), only (004) diffraction peak from the anatase TiO_2 is observed (compared with the PDF #782486). The result suggests that the as-deposited $TiO_{2-\delta}$ film is highly *c*-axis oriented and of single phase which is similar to the TiO_2 films on $LaAlO_3$, $SrTiO_3$, and MgO substrates.[23] The lattice mismatch $(a_{film} - a_{substrate})/a_{substrate}$ along the direction of ⟨100⟩ $TiO_{2-\delta}$ is −5.87%. XRD φ scan measurements were used to establish the in-plane crystallographic orientation of the $TiO_{2-\delta}$ film with respect to that of PMN-PT. The results reveal a good epitaxy of the $TiO_{2-\delta}$ film on the PMN-PT. The in-plane orientation relationships were obtained as ⟨100⟩ $TiO_{2-\delta}$//⟨100⟩ PMN-PT and ⟨010⟩ $TiO_{2-\delta}$//⟨010⟩ PMN-PT.

The inset of Fig. 1 shows the schematic setup for measuring the resistance of the $TiO_{2-\delta}$ film and applying gate voltages across the PMN-PT. Silver electrodes with the width of 0.4 mm were evaporated onto the top surface of the $TiO_{2-\delta}$ film using the predefined shielding mask. The length and width of the $TiO_{2-\delta}$ channel in the FeFET were 1.4 and 3 mm, respectively. The gate electrode was prepared on the backside of the PMN-PT substrate. The gate voltage was supplied across 0.5 mm-thick PMN-PT by a Keithley 6487 voltage source and the resistance was measured by a Keithley 2400 source meter using a two-probe method with a read current of 0.1–1 μA. All the measurements were taken after the PMN-PT substrate was polarized from the original state by applying $E = -10$ kV/cm polarization electric field for 10 min.

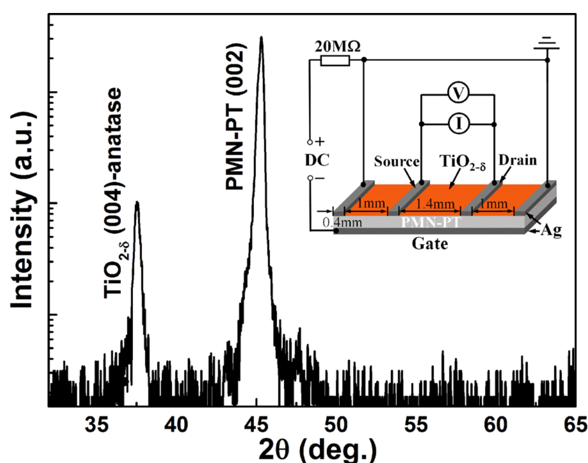

FIG. 1. XRD θ-2θ scan pattern for the $TiO_{2-\delta}$/PMN-PT. Inset: schematic of the structure of the sample, Ag electrodes and circuit for applying gate voltages across PMN-PT and measuring the resistance.

The resistances of the $TiO_{2-\delta}$ film R as a function of gate electric fields E across PMN-PT were measured at room temperature. The sweeping electric field is along $0 \rightarrow +E \rightarrow 0 \rightarrow -E \rightarrow 0$ process marked as (1) → (2) → (3) → (4) in Fig. 2(a). As we can see from Fig. 2, the film resistances could be reversibly modified with the sweeping E and are strongly related to the strength of the electric field E. When the sweeping electric field is small ($E \leq 0.6$ kV/cm), the film resistances change slightly and return to the original state after removing the electric field. While the applying forward electric field is larger than 0.6 kV/cm, the film resistances sharply increase to high-resistance states (HRS or OFF) and maintain in the absence of the electric field. Reverse bias switches the film resistance back to low-resistance states (LRS or ON). Due to the distinct difference in the resistance for the two states at $E = 0$ kV/cm, the on-off ratio is defined as R_{OFF}/R_{ON}. As shown in the figure, with the increase of E, the resistance for HRS becomes larger. When the sweeping electric field is larger than 2 kV/cm (the coercive field of the PMN-PT is ~2 kV/cm), the R versus E curves exhibit rectangle-like hysteresis loops, which is similar to the polarization-electric field hysteresis loop of the PMN-PT substrate.

Figure 3(a) shows dependence of the R_{OFF}/R_{ON} on the peak sweeping electric field E across the PMN-PT. The R_{OFF}/R_{ON} value remains at ~1 under the $E \leq 0.6$ kV/cm and increases to ~3413 with the E increasing to 6 kV/cm. Clearly, the increase of R_{OFF}/R_{ON} as a function of E includes two steps, which we think may be attributed to two different

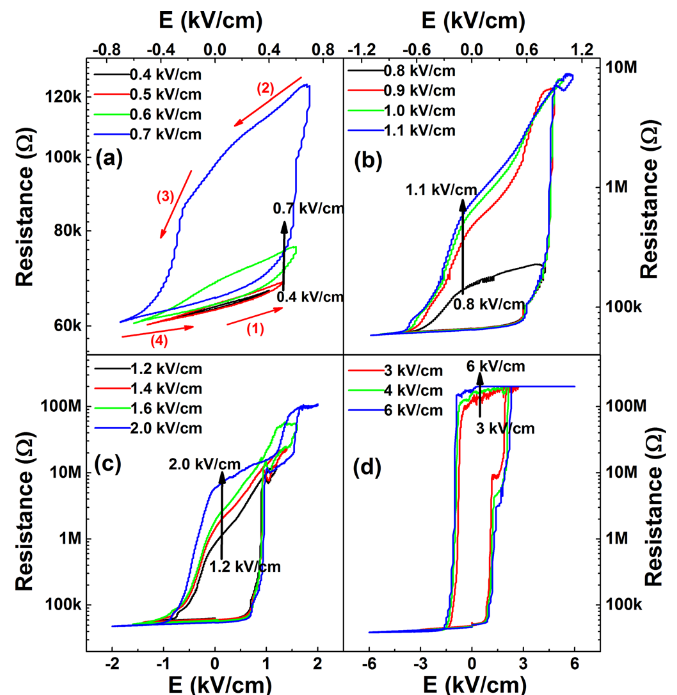

FIG. 2. The resistance of the $TiO_{2-\delta}$ film as a function of one sweeping electric field E cycle along $0 \rightarrow +E \rightarrow 0 \rightarrow -E \rightarrow 0$ [(1) → (2) → (3) → (4)] with different strengths (a) 0.4, 0.5, 0.6, 0.7, (b) 0.8, 0.9, 1, 1.1, (c) 1.2, 1.4, 1.6, 2, and (d) 3, 4, and 6 kV/cm, respectively, across the PMN-PT. The reading current is 1 μA for (a) and (b) and 0.1 μA for (c) and (d). The resistance is beyond the scale of the measuring instrument (over 200 MΩ) in (d).

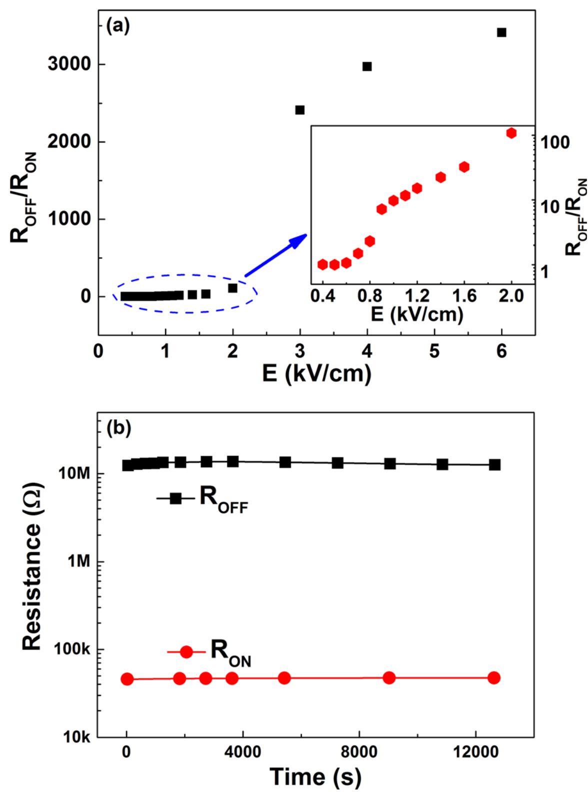

FIG. 3. (a) The dependence of the on-off ratio R_{OFF}/R_{ON} on the electric field E across the PMN-PT; (inset) the illustration for details of the R_{OFF}/R_{ON} under $E \leq 2$ kV/cm. (b) The resistance for the HRS and LRS as a function of time after applying the ±2.5 kV/cm electric field, respectively.

processes. With the E increasing from 0.6 to 2 kV/cm, the R_{OFF}/R_{ON} gradually increases from 1 to 108. When $E > 2$ kV/cm, larger than the coercive field of PMN-PT, the R_{OFF}/R_{ON} dramatically increases to ∼3413 at $E = 6$ kV/cm which is limited by the measuring instrument and could be lager actually. The tunable on-off ratio reveals possibilities for multiple-state data storage. The resistance retentions of $TiO_{2-\delta}$/PMN-PT were measured for 3.5 h in the air of 40%–60% humidity at 300 K. Figure 3(b) shows the time dependence of the resistance at HRS and LRS which are achieved by the $E = \pm 2.5$ kV/cm electric field, respectively. There are no significant changes for the resistance at the HRS and LRS state, indicating the good retention properties for date storage.

To evaluate the stability of the devices, we performed pulse endurance measurements. The results for the $TiO_{2-\delta}$/PMN-PT are shown in Fig. 4(a). HRS/LRS switching is achieved by applying pulsed electric fields of +1.2 kV/cm and −1.2 kV/cm for reset (LRS to HRS) and set (HRS to LRS) operations, respectively. The resistance is then read out with a read current of 1 μA. It is observed that stable HRS and LRS states are achieved with R_{OFF}/R_{ON} of ∼10.5. Figure 4(b) shows the film resistances as a function of positive and negative pulsed electric fields of +1.4 kV/cm and −1.4 kV/cm across the PMN-PT. The stable HRS and LRS states are also achieved with R_{OFF}/R_{ON} of ∼18.

As mentioned above, the multiple-state, reversible, nonvolatile, and reproducible resistive switching behaviors in the $TiO_{2-\delta}$ film are achieved by applying electric fields across the PMN-PT substrate. The R_{OFF}/R_{ON} values observed in the

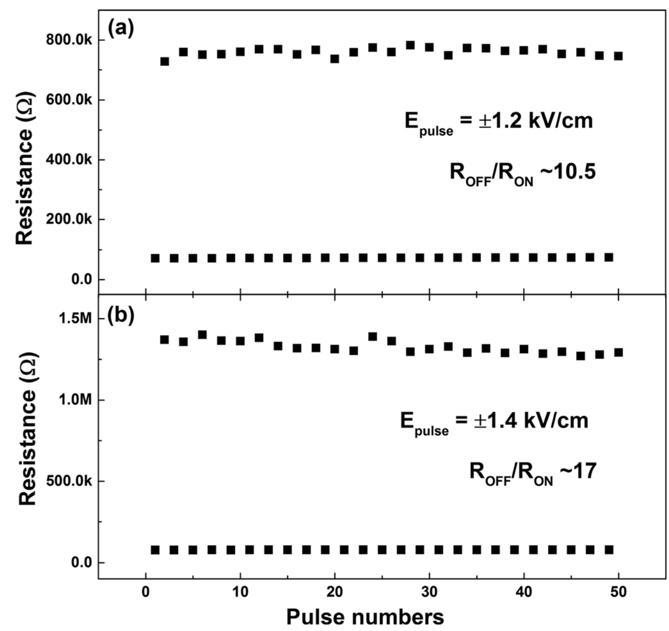

FIG. 4. The film resistances as a function of positive and negative pulsed electric fields across the PMN-PT. The pulse condition for the HRS/LRS is (a) +1.2 kV/cm/−1.2 kV/cm and (b) +1.4 kV/cm/−1.4 kV/cm with a pulse width of 100 ms.

$TiO_{2-\delta}$/PMN-PT are much larger than those of other reported transition-metal oxide film/PMN-PT heterostructures, where the nonvolatile resistivity modulation was achieved through the electric field induced metastable ferroelastic strain. Moreover, different from the nonvolatile resistance modulation based on the ferroelectric field effect, the large relative change of the resistance could also be achieved under the gate electric fields smaller than its coercive electric field, which gives us the different understanding of the mechanism. $TiO_{2-\delta}$ is one of the important materials for investigating the resistive switching behavior and the resistive RAM application. In Metal/$TiO_{2-\delta}$/Metal memory devices, the conductive filament effect and the migration of the oxygen vacancies are the main switching mechanisms to explain the unipolar and the bipolar switching behavior, respectively.[24] In the $TiO_{2-\delta}$/PMN-PT structure proposed in this paper, the set and reset electric fields are applied across the PMN-PT along the thickness direction, showing no contribution to the $TiO_{2-\delta}$ layer along the in-plane measurement direction. Therefore, the nonvolatile switching behavior could be attributed to the migration of the positively charged oxygen vacancies and the ferroelectric field effect induced charge manipulations.

In the $TiO_{2-\delta}$/PMN-PT FeFET structure, the ferroelectric field effect of PMN-PT can significantly change the charge density of the $TiO_{2-\delta}$ film, leading to resistance modulations like normal FeFETs. The $TiO_{2-\delta}$ channel is an n-type material, so the majority of carriers in the channel are electrons. When the PMN-PT was polarized by a negative electric field, the electrons in the $TiO_{2-\delta}$ channel are induced to compensate the positive polarization charges, thereby accumulating the channel of negative electrons and setting the channel resistance to LRS. When the positive gate electric field was applied across the PMN-PT, ferroelectric domains near the interface of PMN-PT will be switched, resulting in the negative polarization charges. This

rearrangement effectively depletes the channel of the electrons and therefore switches the resistance into HRS.

Apart from the charge manipulations by the ferroelectric field effect, the migration of the positively charged oxygen vacancies in the $TiO_{2-\delta}$ film plays an important role in the large multiple-state nonvolatile resistive switching. By applying the gate electric field across the PMN-PT, ferroelectric domains near the interface of PMN-PT will be switched, thereby switching ferroelectric polarization charge. The positively charged oxygen vacancies in $TiO_{2-\delta}$ will be pushed forward/backward by the coulomb force, resulting in an oxygen vacancy poor/rich region near the $TiO_{2-\delta}$ surface as shown in Fig. 5. Metal/semiconductor contacts are typically ohmic in the case of very heavy doping and rectifying (Schottky-like) in the case of low doping.[25] Therefore, when the positive electric field is applied, the contact between the metal electrodes and the oxygen poor region near the surface is Schottky-like. The corresponding equivalent circuit consists of two opposite rectifiers in series leading to HRS, as shown in Fig. 5(a).[26] While under negative electric field, oxygen vacancies accumulate near the surface and the contacts between the metal electrodes and the oxygen vacancy rich region are ohmic. And the corresponding equivalent circuit consists of two small resistances in series leading to LRS, as shown in Fig. 5(b). Owing to the stability of oxygen vacancies after removing the electric field, resistive switching behaviors are nonvolatile. By different strengths of the gate electric field, the ferroelectric domains near the PMN-PT interface and oxygen vacancies near the $TiO_{2-\delta}$ film surface are modulated to a different degree, resulting in the multiple-state nonvolatile resistive switching.

As a result, applying the positive electric field across the PMN-PT, the density of the oxygen vacancy near the surface of $TiO_{2-\delta}$ decreases and also the electron density of the film decreases, which leads to the higher resistance for the HRS states. In contrast, applying the negative electric field, the oxygen vacancy density near the surface of $TiO_{2-\delta}$ increases and the electron density of the film increases, resulting in the lower resistance for the LRS states. Thus, the resistance modulation R_{OFF}/R_{ON} dramatically increases to $\sim$3413 at $E = 6$ kV/cm. Based on the co-operation of the two mechanisms—the migration of oxygen vacancies and the ferroelectric field effect induced charge manipulations, the on-off ratio of the film resistance is much larger than the previous researches.[21,22]

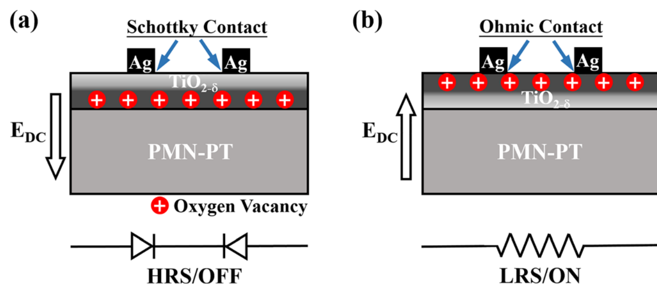

FIG. 5. Junctions between the Ag electrodes and the oxygen-deficient $TiO_{2-\delta}$ film show the role of the interfaces in determining the electrical transport behavior. The schematic diagrams of the migration of oxygen vacancies and the corresponding equivalent circuit for (a) HRS and (b) LRS.

We have studied resistive switching behaviors in the ferroelectric heterostructure $TiO_{2-\delta}$/PMN-PT at room temperature. The resistance of the $TiO_{2-\delta}$ film could be reversibly modulated by applying gate voltage across the ferroelectric PMN-PT. Different from normal FeFETs, the resistance can be reversibly switched into different stable states under different strengths of gate electric field. And the on-off ratio R_{OFF}/R_{ON} tuned by the strength of the electric field provides the opportunity to multiple-state data storage. The large multiple-state nonvolatile resistive switching behaviors is discussed based on the co-operation of the ferroelectric field effect induced charge manipulations and the migration of the positively charged oxygen vacancies. The large, nonvolatile, reproducible and multiple-state resistive switching behaviors in the $TiO_{2-\delta}$/PMN-PT at room temperature present a potential strategy for designing nonvolatile memory devices.

This work has been supported by the National Key Project for Basic Research (No. 2014CB921002), the National Natural Science Foundation of China (Grant Nos. 11504432, 11374225, and 11574227), Shandong Provincial Natural Science Foundation (BS2015DX002), Qingdao Science and Technology Program for Youth (16–5-1–6-jch), and the Research Grant Council of Hong Kong (Project No. HKU 702112P).

[1]C. H. Ahn, J. M. Triscone, and J. Mannhart, "Electric field effect in correlated oxide systems," Nature **424**, 1015 (2003).
[2]J. Hoffman, X. Pan, J. W. Reiner, F. J. Walker, J. P. Han, C. H. Ahn, and T. P. Ma, Adv. Mater. **22**, 2957 (2010).
[3]S. M. Wu, S. A. Cybart, P. Yu, M. D. Rossell, J. X. Zhang, R. Ramesh, and R. C. Dynes, Nat. Mater. **9**, 756 (2010).
[4]H. J. Molegraaf, J. Hoffman, C. A. Vaz, S. Gariglio, D. Van Der Marel, C. H. Ahn, and J. M. Triscone, Adv. Mater. **21**, 3470 (2009).
[5]W. Eerenstein, N. D. Mathur, and J. F. Scott, Nature **442**, 759 (2006).
[6]D. Yi, J. Liu, S. Okamoto, S. Jagannatha, Y. C. Chen, P. Yu, Y. H. Chu, E. Arenholz, and R. Ramesh, Phys. Rev. Lett. **111**, 127601 (2013).
[7]C. A. Vaz, J. Phys.: Condens. Matter **24**, 333201 (2012).
[8]V. Garcia, M. Bibes, L. Bocher, S. Valencia, F. Kronast, A. Crassous, X. Moya, S. Enouz-Vedrenne, A. Gloter, D. Imhoff, C. Deranlot, N. D. Mathur, S. Fusil, K. Bouzehouane, and A. Barthélémy, Science **327**, 1106 (2010).
[9]M. Gajek, M. Bibes, S. Fusil, K. Bouzehouane, J. Fontcuberta, A. E. Barthelemy, and A. Fert, Nat. Mater. **6**, 296 (2007).
[10]D. Pantel, S. Goetze, D. Hesse, and M. Alexe, Nat. Mater. **11**, 289–293 (2012).
[11]C. Thiele, K. Dörr, O. Bilani, J. Rödel, and L. Schultz, Phys. Rev. B **75**, 054408 (2007).
[12]Y. Y. Zhao, J. Wang, H. Kuang, F. X. Hu, H. R. Zhang, Y. Liu, Y. Zhang, S. H. Wang, R. R. Wu, M. Zhang, L. F. Bao, J. R. Sun, and B. G. Shen, Sci. Rep. **4**, 7075 (2014).
[13]Q. X. Zhu, M. Zheng, M. M. Yang, X. M. Li, Y. Wang, X. Shi, H. L. W. Chan, H. S. Luo, X. G. Li, and R. K. Zheng, Appl. Phys. Lett. **103**, 132910 (2013).
[14]Z. G. Sheng, J. Gao, and Y. P. Sun, Phys. Rev. B **79**, 174437 (2009).
[15]E. J. Guo, J. Gao, and H. B. Lu, Appl. Phys. Lett. **98**, 081903 (2011).
[16]M. Liu, J. Hoffman, J. Wang, J. Zhang, B. Nelson-Cheeseman, and A. Bhattacharya, Sci. Rep. **3**, 1876 (2013).
[17]Y. Yang, Z. L. Luo, M. M. Yang, H. Huang, H. Wang, J. Bao, G. Pan, C. Gao, Q. Hao, S. Wang, M. Jokubaitis, W. Zhang, G. Xiao, Y. Yao, Y. Liu, and X. G. Li, Appl. Phys. Lett. **102**, 033501 (2013).
[18]B. Zhi, G. Gao, H. Xu, F. Chen, X. Tan, P. Chen, L. Wang, and W. Wu, ACS Appl. Mater. Interfaces **6**, 4603 (2014).
[19]S. Dong, X. Zhang, R. Yu, J. M. Liu, and E. Dagotto, Phys. Rev. B **84**, 155117 (2011).
[20]J. Hoffman, X. Hong, and C. H. Ahn, Nanotechnology **22**, 254014 (2011).

[21]S. Mathews, R. Ramesh, T. Venkatesan, and J. Benedetto, Science **276**, 238 (1997).
[22]Q. X. Zhu, M. M. Yang, M. Zheng, R. K. Zheng, L. J. Guo, Y. Wang, J. X. Zhang, X. M. Li, H. S. Luo, and X. G. Li, Adv. Funct. Mater. **25**, 1111 (2015).
[23]S. Yamamoto, T. Sumita, A. Miyashita, and H. Naramoto, Thin Solid Films **401**, 88 (2001).
[24]H. S. P. Wong, H. Y. Lee, S. Yu, Y. S. Chen, Y. Wu, P. S. Chen, B. Lee, F. T. Chen, and M. J. Tsai, Proc. IEEE **100**, 1951 (2012).
[25]E. H. Rhoderick and R. H. Williams, *Metal–Semiconductor Contacts*, 2nd ed. (Oxford Science Publications, Oxford, 1988).
[26]J. J. Yang, M. D. Pickett, X. Li, D. A. Ohlberg, D. R. Stewart, and R. S. Williams, Nat. Nanotechnol. **3**, 429 (2008).